Intramolecular Energy Transfer in S_1- and S_2-States of Porphyrin Trimers

Aiko Nakano,[†] Yuzo Yasuda,[†] Tomoko Yamazaki,[‡] Seiji Akimoto,[‡] Iwao Yamazaki,*[,‡] Hiroshi Miyasaka,*[,§] Akira Itaya,[§] Masataka Murakami,[§] and Atsuhiro Osuka*[,†]

Department of Chemistry, Graduate School of Science, Kyoto University, Kyoto 606-8502, Japan, Department of Chemical Process Engineering, Graduate School of Engineering, Hokkaido University, Sapporo 060-8628, Japan, and Department of Polymer Science and Engineering, Kyoto Institute of Technology, Kyoto 606-8585, Japan

Received: February 15, 2001

A set of four porphyrin trimers (**1**−**4**) consisting of an energy-accepting 5,15-diphenylethynyl-substituted Zn(II)-porphyrin core flanked by two energy-donating peripheral Zn(II)-porphyrins have been prepared as a new efficient energy-transfer functional unit. The peripheral porphyrin donor is either a TPP-type Zn(II)-porphyrin for **1** and **2** or a OEP-type Zn(II)-porphyrin for **3** and **4** and the diphenylethynyl substitution axis of the core porphyrin is aligned either orthogonal in **1** and **3** or parallel in **2** and **4** with respect to the long axis of the trimeric arrays. Femtosecond transient absorption spectroscopy and femtosecond up-conversion fluorescence measurement have revealed the very efficient S_1-S_1 energy-transfer reactions in these porphyrin trimers. The S_1-S_1 energy transfer is faster in the parallel trimers **2** and **4** than in the orthogonal trimers **1** and **3**, reflecting larger electronic coupling in the former pair. The peripheral porphyrin S_2-state lifetime is considerably shortened in **1**−**4**, which has been ascribed to S_2-S_2 energy transfer. Probably the strong Soret-transitions of both the donor and acceptor lead to large Coulombic interactions, thereby rendering S_2-S_2 energy transfer effective enough to compete with rapid internal conversion to S_1-state. These results encourage a new strategy for construction of porphyrin-based supramolecular artificial photosynthetic antenna.

Introduction

Many elaborate porphyrin arrays have been synthesized as their potential uses for photonic devices such as light harvesting functional subunits,[1] charge separating subunits,[1,2] a signal-transmitting optical wire,[3a] an optoelectronic gate,[3b] and ultrafast molecular switches,[4] in which porphyrins are directly connected[5] or covalently linked by a variety of conjugated or unconjugated spacers.[6,7] Since the light-harvesting process as well as the signal transmission processes rely on the rate and efficiency of excitation energy transfer process, understanding of the key factors governing the energy transfer is crucial for the realization of truly efficient antenna molecular systems as well as molecular photonic devices. Equally important is the development of a novel efficient energy-transfer functional unit that can rival the key natural energy-transfer components such as carotenoid-to-bacteriochlorophyll[8] and B850 in LH2.[9] Such very fast energy-transfer functional units will be useful in view of their incorporation into supramolecular multi-porphyrin arrays.

The major aim of the present investigation is to construct an effective energy-transfer functional unit that can be easily incorporated into supramolecular photosynthetic model systems. To explore the possibility of driving intramolecular energy transfer from the upper excited state is another challenging goal. Usually, the upper excited states such as S_2 are too short-lived to be involved in energy-transfer or electron-transfer reactions due to extremely rapid internal conversion to the lowest excited singlet state. In the natural photosynthesis, however, it has been now recognized that S_2-states of some carotenoids do play an important role by transferring the captured light-energy to the S_2-state of chlorophyll presumably through dipole−dipole Coulombic interaction.[10] Interestingly, the other biological roles of carotenoids are fulfilled by other excited states; the photoprotective role of dissipating the excitation energy of the triplet chlorophylls is performed by T_1-state of most of carotenoids and the effective light intensity at the reaction center is regulated by S_1-state of some carorenoids.[10,11] Such a multiple use of the pigment will be a next important target of the artificial systems, since it will pave a way for the design and synthesis of a single molecule as a multiply functional component, which must be useful for construction of more sophisticated molecular system close to the natural photosynthetic reaction centers.

In the design of the energy transfer from S_2-states, zinc(II) *meso*-tetraphenylporphyrin (Zn(II)-TPP) is an exceptional molecule since its S_2 state has a relatively long lifetime of 2.4−3.5 ps in various solvents.[12,13] The relatively long lifetime of the S_2-state of Zn(II)-TPP may be ascribed to a large energy gap and poor Franck−Condon factor between the S_2-state and S_1-state. Despite this favorable feature, the realization of energy transfer from the S_2-state has been not straightforward. Energy transfer from the S_2-state of OEP-type β-octaalkyl Zn(II) porphyrin would be more difficult due to its extremely short lifetime.[13d] Nevertheless it is to be noted that the Coulombic interactions between the transition dipole moments should be much larger in the S_2-state of porphyrins owing to the strongly dipole-allowed nature of Soret-transition. However, use of strongly dipole-allowed Soret (S_0-S_2)-transition of porphyrins for realization of the energy transfer from S_2-state has been quite rare.[14] Another important issue in the design of an efficient state-to-state energy transfer is to avoid the exciton coupling case in which the excitation is well delocalized over the donor and

[†] Department of Chemistry.
[‡] Department of Chemical Process Engineering.
[§] Department of Polymer Science and Engineering.

10.1021/jp010596s CCC: $20.00
Published on Web 05/01/2001

acceptor. Furthermore, deleterious electron-transfer quenching reactions should be also avoided in the molecular design.

On the other side, ultrafast laser technology has been expanding the temporal region we can access and has allowed the measurement of extremely fast energy-transfer reactions. Actually, several examples have been reported on the electron transfer and energy transfer from the upper excited states in recent years.[11,13,14] Here, we used the femtosecond transient absorption spectroscopy and fluorescence up-conversion measurement.

In this paper, we examined the singlet−singlet energy-transfer processes in four trimeric porphyrin arrays **1**−**4** with a particular intention of exploring the energy transfer from the S_2- excited state. It is interesting to note that such energy transfer from S_2-excited state would be very difficult for frequently studied Zn(II)—free base hybrid diporphyrins,[1−3,7] since there is only little energy difference between the two S_2-states. In this sense, *meso*,*meso*-bisphenylethynyl substituted Zn(II) porphyrin is an attractive energy acceptor unit, since its S_2-state is lying substantially lower than that of the normal Zn(II)-porphyrin.[15] Recently *meso*-ethynyl-substituted porphyrins have been extensively studied by Therien,[15] Arnold,[16] Milgrom,[17] Anderson,[18] and other several groups,[19] due to their fascinating optical and electrochemical properties. The lower lying S_1-state of Zn(II) *meso*-ethynyl-substituted porphyrins is also interesting in light of the energy transfer in the S_1-state manifold. Nevertheless, only scattered attention has been paid to the use of this component as an energy acceptor toward normal Zn(II)-porphyrins even in the S_1-state manifold.[20]

Results

Molecular Design and Synthesis. The structures of porphyrin trimers **1**−**4** and reference molecules **5**, **6**, and **7** are shown in Chart 1. The trimers consist of an energy-accepting Zn(II) 5,-15-diphenylethynyl-substituted porphyrin core flanked by two energy-donating peripheral Zn(II)-porphyrins. To examine the effect of the connectivity of the diethynyl-linked porphyrin core with the peripheral porphyrins, the diphenylethynyl-substitution axis of the core porphyrin is set orthogonal with respect to the long trimer axis in **1** and **3** and parallel in **2** and **4**. Energy transfer from S_2-state is more conceivable in **1** and **2** owing to a longer lifetime of the S_2-state of Zn(II)-TPP type energy donor.[12,13] Comparison of the energy-transfer reactions between **1** vs **3** and **2** vs **4** would provide insight into the effects of the porphyrin orbital characteristics in controlling the energy-transfer processes.[21]

The synthesis of the models **1** and **3** is shown in Scheme 1. We employed synthetic routes involving Cu(II) complexes **11**−**13** by following two reasons. First the acid-catalyzed condensation of formyl-substituted porphyrin **10** with 2,2′-dipyrrylmethane led to a very poor yield of porphyrin trimer, probably due to strongly electron accepting property of protonated free base porphyrin that reduces the reactivity of the formyl group. This effect may be mitigated by using an appropriate metal complex such as **11**.[6u] Second, NBS-bromination of porphyrin trimers was quite troublesome for all Zn(II) complexes, particularly in the case of β-octaalkyl-substituted porphyrins. Actually, the NBS-bromination of all zinc-metalated compound **19** led to extensive decomposition.[5e] The electron rich peripheral Zn(II) β-octaalkylporphyrin seemed to be unstable under these bromination conditions. This obstacle may be also circumvented with trimers bearing two peripheral Cu(II)-porphyrins such as **12** and **16**. Therefore, formyl-substituted Cu(II)-porphyrin **11**[22] prepared by the known procedure was condensed[23,24] with 2,2′-dipyrrylmethane[25] to provide 1,4-phenylene-bridged porphyrin trimer **12**. Attachment of two ethynylphenyl group at the central *meso*-position was carried out by following the Therien's procedure.[24] NBS-bromination of **12** gave dibromide **13**, which was converted into all Zn(II)-metalated trimer **14** via demetalation and remetalation with $Zn(OAc)_2$ with an overall yield of 45% from **12**. Subsequent Pd(0)-catalyzed Sonogashira coupling reaction[26] of **14** with phenylacetylene gave **1** in 60% yield. Trimer **3** was prepared via the similar route.

CHART 1: R = C_6H_{13}, Ar_1 = 3,5-Dioctyloxyphenyl, and Ar_2 = 3,5-Di-*tert*-butylphenyl

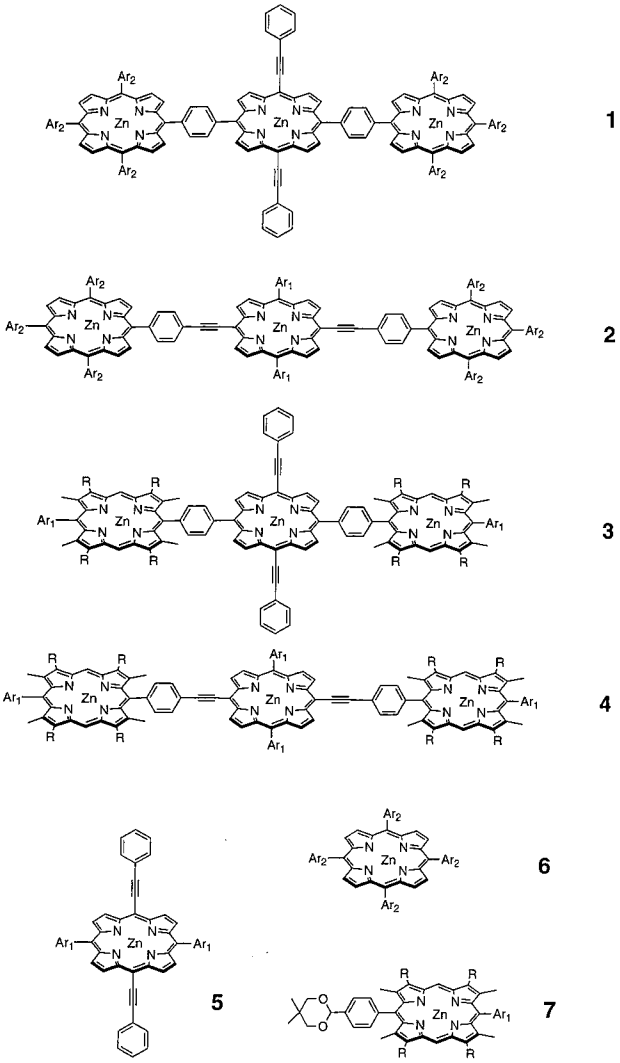

The synthesis of the models **2** and **4** is shown in Scheme 2, where Pd(0)-catalyzed coupling reaction of 4-ethynylphenyl-substituted porphyrins (**22** or **24**) with 5,15-diiodo porphyrin **21** provided **2** and **4** in 60 and 57% yield, respectively.[27] In these coupling reactions, homo-coupled dimers **23** and **25** were formed as a side product. The 5,15-diiodo porphyrin **21** was prepared by *meso*-iodination with the combined use of $AgPF_6$, I_2, and pyridine.[20] Compounds **5**−**7** were also prepared as reference molecules. All the compounds were fully characterized by 500 MHz ^{1}H NMR and FAB MS and MALDI-TOF MS methods.

Absorption and Fluorescence Spectra. Figure 1A shows the absorption spectra of **1**, **5**, and **6** along with a simple absorbance sum of **5** and **6** (1:2) taken in THF. The absorption spectrum of the diphenylethynyl-linked porphyrin **5** shows a red-shifted Soret band at 449 nm ($S_0 \rightarrow S_2$-transition) and

SCHEME 1: Synthesis of 1 and 3[a]

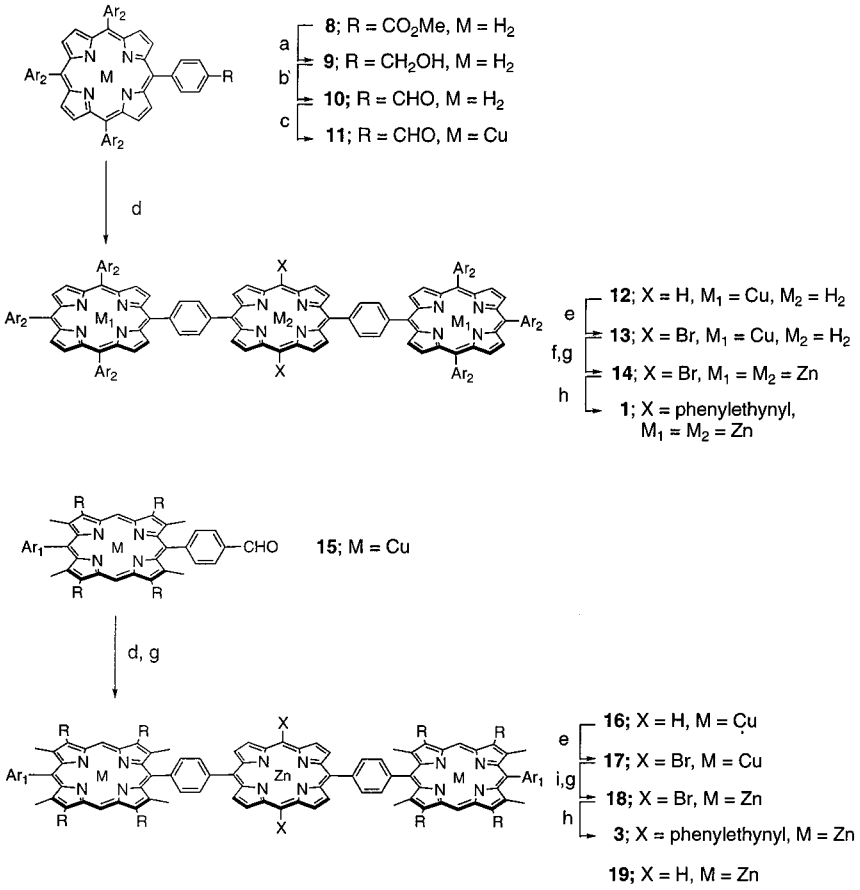

[a] R = C_6H_{13}, Ar_1 = 3,5-dioctyloxyphenyl, and Ar_2 = 3,5-di-*tert*-butylphenyl. Conditions: (a) $LiAlH_4$, THF; HCl; (b) PCC; (c) $Cu(OAc)_2$; (d) 2,2′-dipyrrylmethane, TFA, CH_2Cl_2; DDQ; (e) NBS, $CHCl_3$, pyridine; (f) TFA, (g) $Zn(OAc)_2$; (h) Phenylacetylene, $Pd(PPh_3)_2Cl_2$, CuI, toluene, Et_3N; (i) TFA, 10% H_2SO_4, CH_2Cl_2.

Q-bands at 595 and 649 nm ($S_0 \rightarrow S_1$-transition) as reported previously.[15] A *meso*-ethynyl group provides a strong effect to porphyrin π-conjugated ring, and the conjugation is well expanded over the diphenylethynyl substituents, resulting in the removal of the degeneracy of the porphyrin e_g LUMO orbital. This effects the *x*- and *y*-polarized transitions inequivalent and intensifies the quasi-allowed Q-band by intensity-borrowing from the Soret-transitions.[28] In fact, the Soret band is broader (fwhm = 735 cm^{-1}) in THF at room temperature and becomes a clearly split band at 453 and 461 nm at 77 K in MTHF matrix. Both of the S_1-state and S_2-state of 5,15-diphenylethynyl-substituted Zn(II) porphyrin are lying, respectively, at lower energies in comparison to those of the TPP-type Zn(II)-porphyrin like **6** (Table 1). The linear analysis of the absorption spectrum of **1** in terms of a simple sum of the appropriate models indicates that the Q-bands are negligibly affected when the pigments are linked to form this array, whereas the perturbation of the Soret-bands is substantial. In the absorption spectrum of **1**, the Soret band of the diphenylethynyl-linked porphyrin is observed as a split band at 449 and 462 nm, probably through the exciton interaction with the peripheral porphyrins. The Soret band of the peripheral porphyrins is observed as a single band at 424 nm, being nearly the same wavelength of **6** (425 nm), but its bandwidth is certainly spread (fwhm = 655 cm^{-1}) than that (fwhm = 465 cm^{-1}) of **6**.

The absorption spectrum of **2** is different from that of **1**, in that the Soret band of the diphenylethynyl-linked porphyrin is observed as a broad single band at 455 nm and its Q-band is 8 nm red-shifted and intensified in comparison to that of **5** (Figure 2A). The absorption spectrum of **3** displays a split Soret band at 449 and 459 nm and unperturbed Q-band for the diphenylethynyl-linked porphyrin at 651 nm (Figure 3A), while the absorption spectrum of **4** displays an intensified single Soret band at 455 nm and a red-shifted and intensified Q-band at 658 nm for the diphenylethynyl-linked porphyrin (Figure 3B). From the analysis of the absorption spectra, it is interesting to note that we can selectively excite the energy donor porphyrin at 540−560 nm into its S_1-state or at 400−430 nm into its S_2-state in **1**−**4**.

Figure 1B shows the steady-state fluorescence spectra of **1**, **5**, and **6** taken for excitation at 550 nm. Concentrations were adjusted to be 1×10^{-6} M for **1** and **5** and 2×10^{-6} M for **6**. Excitation into 550 nm corresponds to preferential population of the S_1-state of the peripheral porphyrin energy donor but the fluorescence of **1** is only coming from the S_1-state of the diphenylethynyl-linked porphyrin unit with almost complete fluorescence quenching of the peripheral porphyrins, indicating efficient S_1-S_1 energy transfer. Upon excitation of the above solutions of **1** and **5** at 550 nm, the fluorescence intensity of **1** was ca. 7.5 times larger than that of **5**, indicating that the absorbed light by the peripheral porphyrins is transferred to the core porphyrin. The steady-state fluorescence spectrum of **2** shown in Figure 2B also exhibits that the emission is coming only from the diphenylethynyl-linked porphyrin and the fluorescence intensity of **2** is ca. 13 times larger than that of **5**. The observed red shift of the fluorescence peak is in line with its red-shifted Q-band. The trimers **3** and **4** also exhibit the

SCHEME 2: Synthesis of 2 and 4[a]

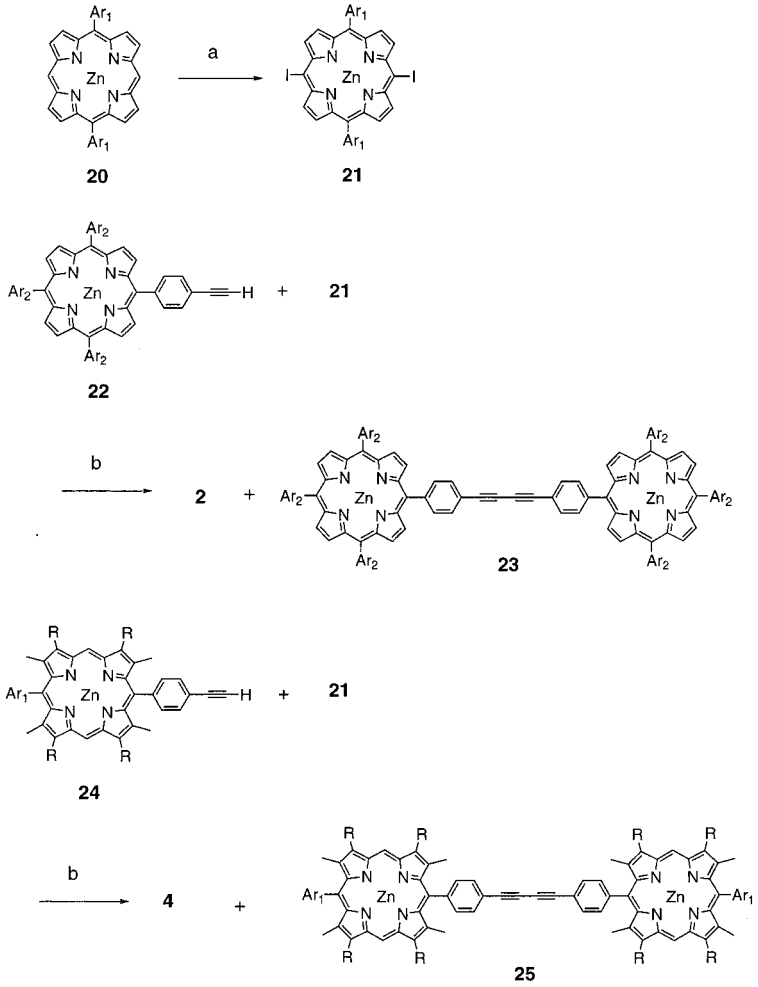

[a] R = C_6H_{13}, Ar_1 = 3,5-dioctyloxyphenyl, and Ar_2 = 3,5-di-*tert*-butylphenyl. Conditions: (a) I_2, $AgPF_6$, pyridine, $CHCl_3$; (b) $Pd(PPh_3)_2Cl_2$, CuI, toluene, Et_3N.

fluorescence spectra only coming from the diphenylethynyl-linked porphyrin core (Figure 3A,B, insets), indicating the occurrence of the similarly efficient S_1-S_1 energy transfer.

Estimation of Energy Levels. Table 1 summarizes the absorption and fluorescence data and the estimated energy levels of the excited singlet states of the chromophore. The energies of the S_1-states were determined from the midpoint of the fluorescence and absorption (0,0) band. The energies of the S_2-states were estimated solely from the absorption data. On the basis of these estimations, energy diagrams can be predicted for the all trimers as shown in Scheme 4. In addition to the S_1-S_1 energy transfer, there is also a substantial energy gradient from the peripheral porphyrin donor to the diphenylethynyl-linked porphyrin acceptor in the S_2-state manifold, which may allow the S_2-S_2 energy transfer in **1**−**4**.

Transient Absorption Spectroscopy. As described above, the steady-state fluorescence spectra of **1**−**4** taken for selective excitation at the peripheral porphyrin exhibit the emission only coming from the diphenylethynyl-linked porphyrins, indicating the S_1-S_1 energy transfer. Fast dynamics of the S_1-S_1 energy transfer were first studied by the transient absorption spectroscopy.[29] To minimize the effects of the solvent dynamics and relaxation processes, all the ultrafast measurements were carried out in benzene solutions. Figure 4 shows the transient absorption spectra of **5**, **6**, and **7** at 100 ps delay time taken for excitation at 532 nm. The spectrum of **5** shows positive absorbance at 480 nm due to the $S_1 \rightarrow -S_n$ absorption and strong bleaching at 640 nm due to the ground-state Q absorption band and a broad dip around 710 nm due to the induced emission in accord with the previous study.[15c] In an analogous manner with the related molecules,[30,31] the spectrum of **6** shows positive absorbance at 455 nm and bleachings at 550 and 590 nm and a broad dip around 650 nm, and that of **7** shows positive absorbance at 460 nm and bleaching at 540 and 575 nm and a broad dip at 640 nm, respectively. Figure 5 shows the transient absorption spectra of **1**−**4** at 20 ps delay time upon excitation at 532 nm. Although the excitation at 532 nm results in selective population of the peripheral porphyrin donor, the transient absorption spectra of **1**−**4** revealed strong bleaching at 640 ∼ 650 nm due to depletion of the ground-state diphenylethynyl-substituted porphyrin core, indicating the energy transfer. In addition, bleachings due to the Q-bands of the peripheral porphyrin energy donors were observed distinctly in the transient spectra of **3** and **4**.

To obtain the rates of S_1-S_1 energy transfer, the femtosecond kinetic measurements were applied for the transient absorbance. As the pump source, the 540−560 nm laser pulse was used for the selective excitation of the peripheral porphyrin donor. Time profiles were monitored at 540−550 nm (the Q-bands of the energy donor and the positive absorbance due to S_1-state of the energy acceptor) and at 640−660 nm (the Q-bands of the energy acceptor). The pulse duration obtained by the cross correlation between pump and probe pulses at the sample position was 0.16 ps.

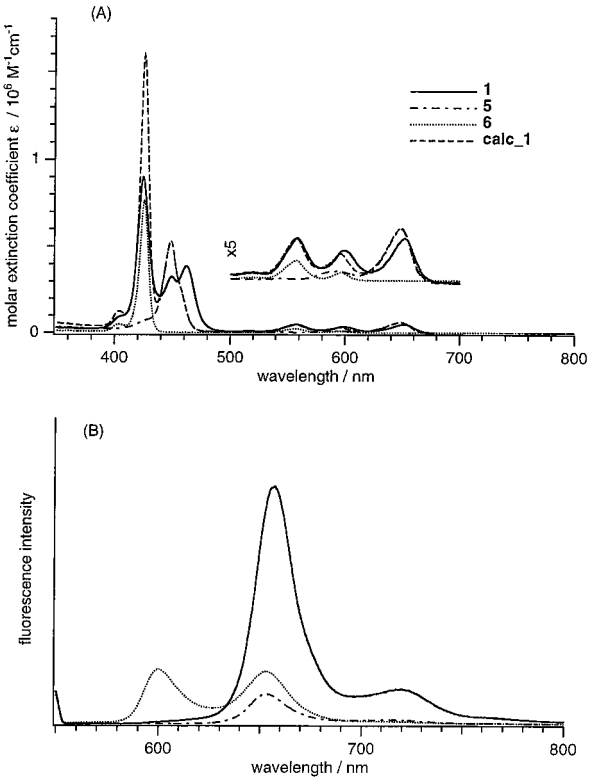

Figure 1. Absorption (A) and fluorescence (B) spectra of **1** and its reference compounds in THF. A simple absorption sum of **5** and **6** (1:2) is also shown as **calc_1**. Fluorescence spectra are taken for excitation at 550 nm. Concentrations are 1×10^{-6} M for **1** and **5** and 2×10^{-6} M for **6**.

Figure 6 shows the time profile of the transient absorbance of **1** excited at 550 nm and monitored at 545 and 640 nm. The time profile monitored at 545 nm shows the slight negative absorbance around the time origin, followed by the increase of the positive signal. As mentioned above, this slight negative absorbance around the time origin corresponds to the bleaching due to the peripheral porphyrin energy donor and the positive absorbance is due to the S_1-state of the acceptor. Since the time profile around the time origin involves the signal due to the coherent artifact, which is phenomenologically attributed to the four-wave mixing, the analysis of the time profile was performed for the time region longer than ca. 0.3 ps following the time origin at the present investigation. A rising time constant at 545 nm was obtained to be 1.6 ps on the basis of the first-order kinetics. The time profile monitored at 640 nm shows that the instantaneous appearance of the transient absorbance is followed by the decrease with a time constant of 1.4 ps. In contrast, the transient absorption signal of the reference acceptor **5** showed no such temporal evolution in this time region. With these results of the kinetic transient absorption measurements and the fluorescence lifetime (1.7 ps) of the peripheral porphyrin donor as described below, we assigned the peripheral porphyrin S_1-state lifetime (τ_{S1}) to be 1.4−1.7 ps. On the basis of these results, we have calculated the rate constant of the S_1-S_1 energy transfer, k_1, by using eq 1:

$$k_1 = 1/\tau_{S1} - 1/\tau_{S1}{}^0 \qquad (1)$$

where $\tau_{S1}{}^0$ is the lifetime of the S_1-state of the reference porphyrin, for which we used the S_1-state lifetime of **6** (2.1 ns).

Similar analysis of the time profiles of the transient absorbance of **2** at 540 and 640 nm (Supporting Information Figure S1) was performed for the time region longer than ca. 0.3 ps in order to avoid the overlap of the coherent artifact signal. The transient absorption signal at 540 nm increases with a time constant of 0.56 ps and a time constant of 0.44 ps was obtained for the growth of the bleaching signal at 640 nm which corresponds to depletion of the core porphyrin ground state. Since the fluorescence lifetime of the donor moiety is 0.45 ps as will be described below, the time constant of 0.44−0.56 ps has been assigned to the S_1-S_1 energy transfer in **2**. Examining both the time profiles of the energy donor and acceptor in a similar manner, the time constants for the S_1-S_1 energy transfer have been determined to be 5.0−6.0 ps and 0.75−0.84 ps for **3** and **4**, respectively (Supporting Information, Figures S2 and S3). The rates of the energy transfer rates calculated by eq 1 are listed in Table 2. We used 1.45 ns of the S_1-state lifetime of **7** as $\tau_{S1}{}^0$ in the calculation of k_1 for **3** and **4**.

Fluorescence Lifetime Measurements. As shown in the previous section, the energy transfer evens in the S_1-state take place in the time region ≪10 ps. Hence, the femtosecond up-conversion method[32] was mainly used for their direct detection. This measurement used the laser pulses with 80-fs pulse width in the range of 390−420 nm, which pumped the peripheral porphyrin donors into their S_2-state and allowed us to observe the subsequent excited-state dynamics. In the case of **1**, the energy donor is a TPP-type Zn(II)-porphyrin which is known to have S_2-S_0 fluorescence emission around 430−450 nm and S_1-S_0 fluorescence emission at 600 nm, and the energy acceptor is a Zn(II) 5,15-diphenylethynyl-substituted porphyrin which has S_1-S_0 emission at 647 nm. Although S_2-S_0 fluorescence emission of the acceptor is not detected in the steady-state fluorescence spectrum, it is expected to appear at the mirror image of the strong Soret band, thus around 480−500 nm, which has been actually monitored by the present femtosecond time-resolved fluorescence measurements.

Figure 7A shows the fluorescence time profile at 460 nm which corresponds to the S_2-S_0 fluorescence of the TPP-type peripheral porphyrin donor in the trimer **1**. The time profile was satisfactorily fit with a biexponential function of a rise component with $\tau = 0.05$ ps and a decay component with $\tau = 0.15$ ps.[33] Considerably shortened S_2-state fluorescence lifetime suggested the energy transfer occurring from the S_2-state. At 500 nm (the S_2-emission of the acceptor), the fluorescence decay profile at 500 nm was analyzed in terms of a biexponential function of a rising component of 75 fs and a decaying component of 0.15 ps. The 0.15 ps time constant was again observed as a decaying component instead of the rising one (Supporting Information, Figure S4A). Failure of the observation of a rising component with $\tau = 0.15$ ps at 500 nm may be explained in terms of (1) there is still substantial overlap of the S_2-S_0 emission of the energy donor and the decaying amplitude is larger than the rising component or (2) the depleting rate of the acceptor S_2-state is larger than its formation rate, which causes a formation time constant of the acceptor S_2-state to be observed as a decaying component. The lifetime of the S_2-emission of **5** at 470 nm has been determined to be ca. 0.46 ps by the fluorescence up-conversion method, and it is plausible that the S_2-state of the diphenylethynyl porphyrin acceptor in **1** may have an additional energy transfer channel to the S_1-state of the peripheral TPP-type porphyrin (k_{21}, Scheme 4) or accelerated internal conversion to the S_1-state (k_{A2}, Scheme 4), eventually decaying with a time constant larger than its formation time constant. Although the analysis of these very

TABLE 1: Absorption and Fluorescence Data in THF

			S_2-state level[a]/eV		S_1-state level[a]/eV	
compounds	absorption data/nm	fluorescence data/nm	donor	acceptor	donor	acceptor
1	424, 449, 462, 558, 599, 651	656, 716	2.92	2.68	2.07	1.90
2	425, 455, 558, 598, 657	654	2.92	2.73	2.07	1.90
3	416, 449, 459, 546, 581, 651	655	2.97	2.70	2.13	1.99
4	416, 455, 546, 580, 658	663, 726	2.97	2.73	2.13	1.88
5	449, 595, 649	654, 715		2.74		1.90
6	425, 556, 596	600, 652	2.92		2.07	
7	416, 546, 578	583, 637	2.97		2.13	

[a] The energy levels of the S_2- and S_1-states are estimated on the basis of the fluorescence and absorption data.

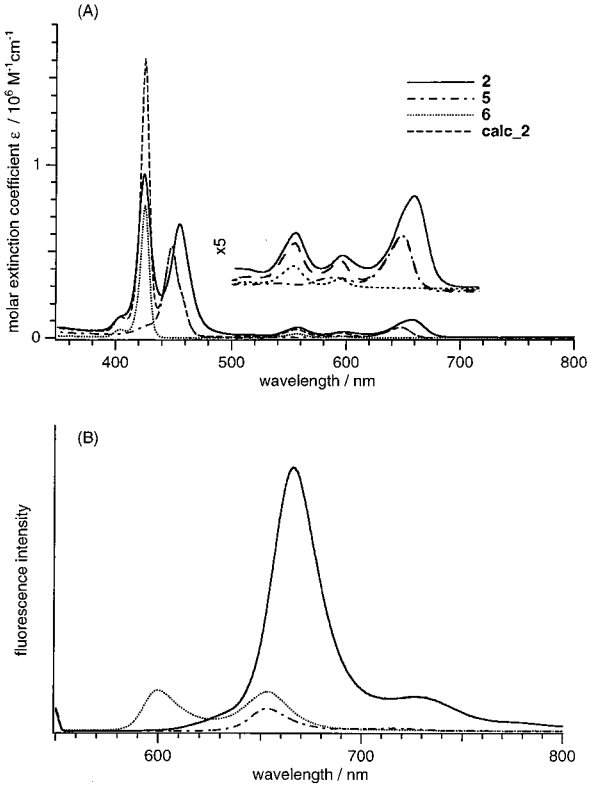

Figure 2. Absorption (A) and fluorescence (B) spectra of **2** and its reference compounds in THF. A simple absorption sum of **5** and **6** (1:2) is also shown as **calc_2**. Fluorescence spectra are taken for excitation at 550 nm. Concentrations are ca. 1×10^{-6} M for **2** and **5** and 2×10^{-6} M for **6**.

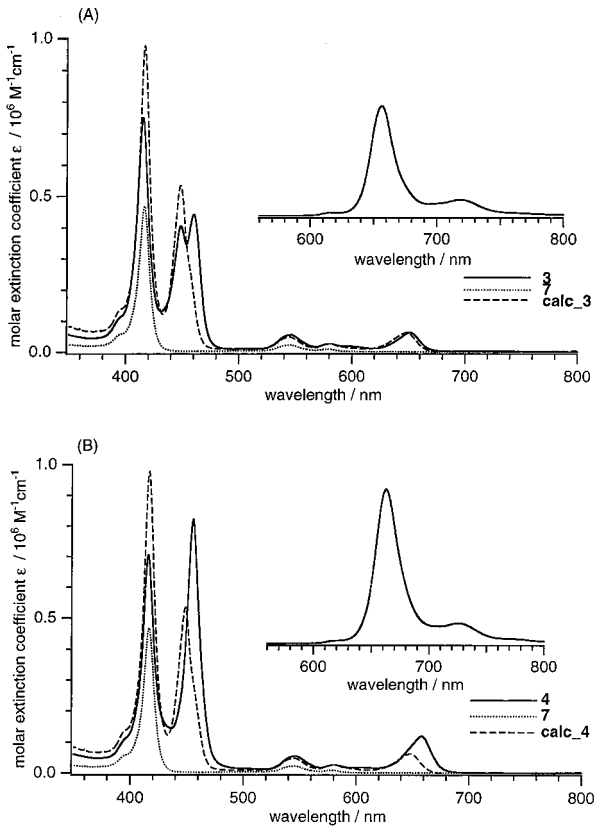

Figure 3. Absorption and fluorescence (inset) spectra of **3** (A) and **4** (B) along with their reference (**7**) and calculated spectrum (**calc_3**, **calc_4**, **5**+**7**, 1:2) in THF. Fluorescence spectra are taken for excitation at 550 nm.

fast excited-state dynamics is complicated, we interpreted here the 0.15 ps time constant for the S_2-lifetime of the peripheral donor.

Figure 7B shows the fluorescence decay of **1** at 600 nm, which corresponds to the emission mainly from the S_1-state of the peripheral TPP-type porphyrin donor. The fluorescence decay curve was analyzed on the assumption that the fluorescence decay should contain the rise and decay components of the S_2-state emission, since the decay curve was obtained by excitation into the S_2-state. Accordingly, the fluorescence decay was deconvoluted with a sum of four exponential functions with the two lifetimes fixed. Obtained results are summarized in Table 3. The main decaying component has a 1.7 ps time constant, which is consistent with the transient absorption result of a 1.4 $\sim$ 1.6 ps time constant. The main rising component of the fluorescence at 710 nm which corresponds to the emission from the S_1-state of the acceptor porphyrin has a 1.5 ps time constant (Supporting Information, S4B).

The fluorescence of **2** was monitored at 450, 500, 600, and 710 nm in the similar manner (Table 3, Supporting Information, Figure S5). The fluorescence decay at 450 nm (Figure S5A) which can be nicely fit with a single-exponential function with $\tau = 0.14$ ps has been assigned to the lifetime of the peripheral porphyrin S_2-state. A time constant of 0.45 ps was found both in the fluorescence decay at 600 nm as a decaying component (Figure S5B) and at 710 nm as a rising component (Figure S5C). This time constant has been assigned to the S_1-S_1 energy transfer, since it is in reasonable accordance with the results obtained by the transient absorption spectroscopy (0.45 $\sim$ 0.56 ps).

On the basis of the obtained lifetimes, we have calculated the rates of the S_2-S_2 energy transfer in **1** and **2** by eq 2:

$$k_2 = 1/\tau_{S2} - 1/\tau_{S2}^{0} \qquad (2)$$

where τ_{S2} is the lifetime of the S_2-state of the energy donor in the trimers and τ_{S2}^{0} is the lifetime of the S_2-state of the reference porphyrin (1.4 ps, for **6**).[34] Calculated rate constants are 6.1×10^{12} and 6.4×10^{12} s^{-1} for **1** and **2**, respectively.

SCHEME 3: Exciton Coupling at the Soret Bands: (A) Trimer 3 and (B) Trimer 4

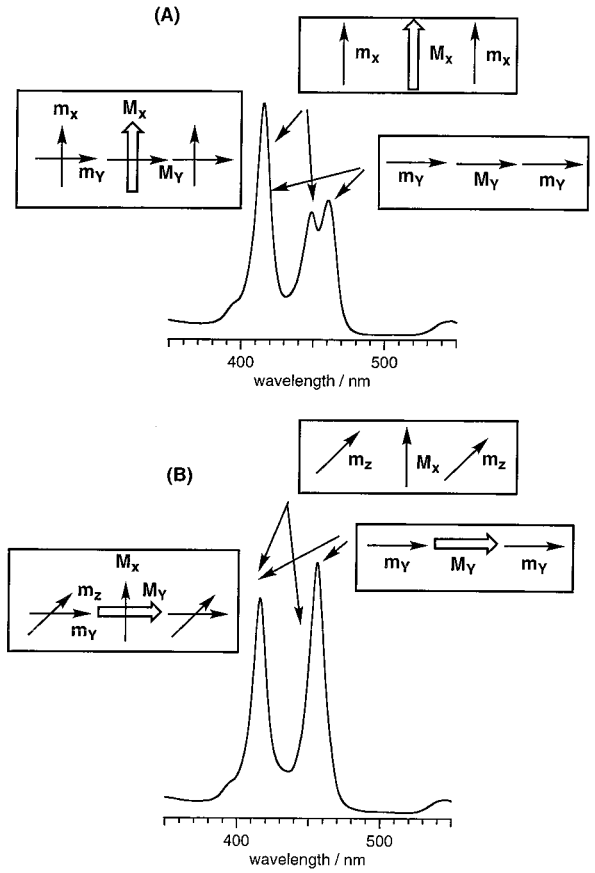

SCHEME 4 : Energy Diagram and Energy-Transfer Scheme: (D) the Energy Donating Peripheral Porphyrin and (A) the Energy Accepting Central Porphyrin

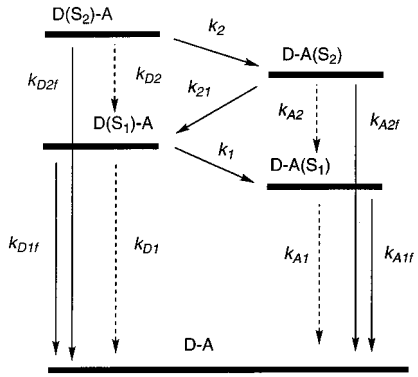

While the trimers **1** and **2** have a TPP-type Zn(II)-porphyrin energy donor with relatively long S_2-lifetime, it is curious to examine the possibility of similar S_2-S_2 energy-transfer reactions in **3** and **4** bearing an OEP-type Zn(II)-porphyrin energy donor which has an extremely short S_2-lifetime. Recently, we determined the S_2-state lifetime of 5,15-diaryl-β-octaalkyl Zn(II) porphyrin like **6** to be ca. 0.15 ps in benzene solution by the fluorescence up-conversion measurement.[13d] Deconvoluted results of the fluorescence decays of **3** and **4** (Supporting Information, Figures S5 and S6) were also summarized in Table 3. The fluorescence decays of **3** at 430 nm and **4** at 450 nm, which correspond to the peripheral porphyrin S_2-state, can be fit with a single-exponential function of $\tau = 0.07$ ps and $\tau = 0.12$ ps, respectively (Supporting Information, Figures S6 and S7). These time constants are somewhat shorter than the reference S_2-state lifetime of 0.15 ps, suggesting the energy transfer in the S_2-state.

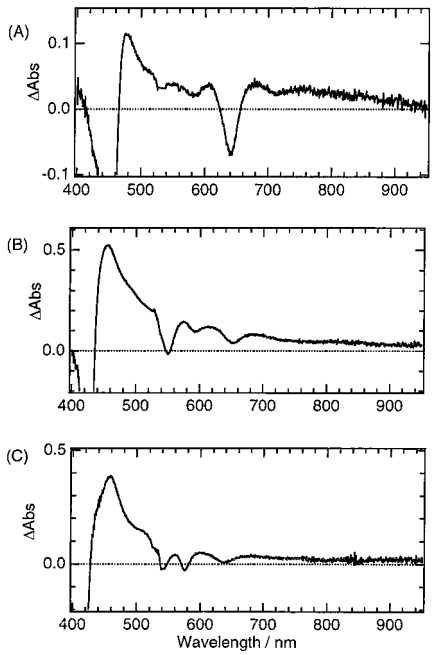

Figure 4. Picosecond transient absorption spectra of **5** (A), **6** (B), and **7** (C) at 100 ps delay time taken for excitation at 532 nm in benzene.

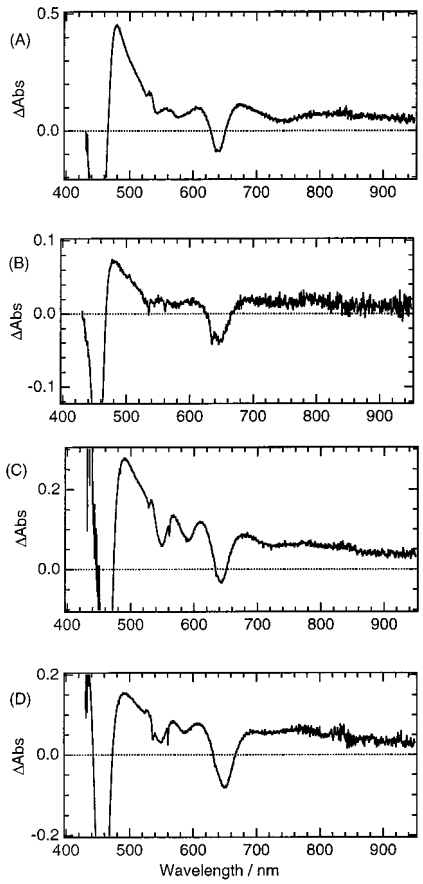

Figure 5. Picosecond transient absorption spectra of **1** (A), **2** (B), **3** (C), and **4** (D) at 20 ps delay time taken for excitation at 532 nm in benzene.

Discussion

The energy-transfer processes can be roughly classified into three cases depending on the magnitude of the electronic

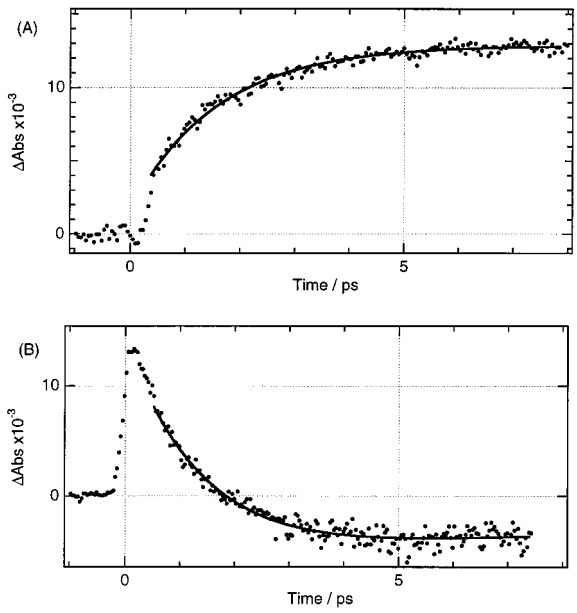

Figure 6. Time-profiles in femtosecond transient absorption spectra of **1**. (A) $\lambda_{ex} = 550$ nm, $\lambda_{obs} = 545$ nm, fitting with $\tau = 1.6$ ps, (B) $\lambda_{ex} = 550$ nm, $\lambda_{obs} = 640$ nm, fitting with $\tau = 1.4$ ps.

coupling between a donor and an acceptor: (1) the strong coupling case, (2) the intermediate coupling cases, and (3) the limit of the weak coupling case.[35] The strong coupling corresponds to the exciton case where the Franck−Condon state of the donor is well distributed over the acceptor and thus the spectra of the donor and acceptor are significantly influenced. In the limit of the weak coupling case known as the Förster mechanism, the energy transfer occurs after completing the vibrational relaxation in the excited-state manifold.[36] The intermediate coupling cases may be further categorized into two; one is the partial exciton case in which the energy transfer occurs with partly retaining the oscillatory coherent feature but quickly loses its coherence due to incoherent perturbations such as collisions and vibrations, and the other one is the hot transfer mechanism in which the energy transfer occurs incoherently during the vibrational relaxation.[35,37] We cannot observe a state-to-state energy transfer in the exciton case.

The electronic coupling can be provided by Coulombic interaction and electron exchange interaction, although the relative contributions differ case by case.[36,38] The Coulombic interaction can be approximated in terms of dipole−dipole interaction for donor−acceptor pairs with sufficiently large separations, resulting in the Förster eq 3:[36]

$$k = \frac{8.8 \times 10^{-25} \kappa^2 \Phi}{n^4 R^6 \tau} \tag{3}$$

$$J = \int F(\upsilon)\epsilon(u)\upsilon^{-4} \mathrm{d}\upsilon \tag{4}$$

in which n is the refractive index of the solvent, R is the center-to-center distance between donor and acceptor, Φ is the fluorescence quantum yield of the donor, τ is the fluorescence lifetime of donor, and κ is a dipole−dipole orientation factor. Also, J is the spectral overlap integral, $F(\nu)$ is the normalized fluorescence spectrum of the energy donor, and $\epsilon(\nu)$ is the absorption spectrum of the energy acceptor with molar extinction coefficient ($M^{-1}cm^{-1}$) unit. Only through-space interaction is taken into account in the Förster mechanism. On the other hand, the electron exchange interactions can be provided through short-range direct orbital overlap or over relatively long distances through an indirect electronic coupling involving lower lying molecular orbitals of the spacer that bridges a donor and an acceptor.[38] In covalently linked donor−acceptor pairs, the electronic exchange interaction is usually mediated by through-bond coupling.[39] In this indirect and mediated case, the electronic coupling depends on the energy level of unoccupied orbital of the spacer as well as on the orbital characteristics of the donor and acceptor involved in the energy transfer, particularly at the atoms attached to the spacer. Lindsey et al. have synthesized various porphyrin arrays using 5,10,15,20-tetraphenylporphyrin (TPP) type components linked by *p,p′*-diarylethyne linker at the porphyrin *meso*-positions and have presented interesting results on the effect of the porphyrinic molecular orbitals on the energy transfer rate.[21]

Important information on the electronic coupling between the donor and acceptor is obtained by the examination of the absorption spectra. We thus first discuss the absorption spectra of **1**−**4**. It is apparent that the absorption spectra are similar for **1** and **3** and for **2** and **4**, indicating that the connectivity of the diphenylethynyl porphyrin core in the trimeric arrays is a dominant factor for their spectral characteristics. The absorption spectra of **1**−**4** can be qualitatively explained in terms of the exciton coupling theory[35] as follows. When we consider two pairs of two transition dipole moments, m_x and m_y for the peripheral porphyrin, and M_x and M_y for the central porphyrin, which are respectively perpendicular and parallel to the long molecular axis of the trimer (Scheme 3). In **1** and **3**, M_x that is along the diphenylethynyl substituents and thus perpendicular to the long axis of the trimers should be larger than M_y. Mutual exciton coupling between m_x and M_x leads to blue shift and that between m_y and M_y leads to red shift, thereby giving rise to a split band, while the other dipole−dipole interactions (m_x and M_y, and m_y and M_x) should be canceled due to the orthogonal arrangements. In comparison of the exciton coupling of m_x and M_x versus m_y and M_y, the former coupling should be orientationally weaker but the oscillator strength of M_x is larger than that of M_y, giving rise to a split Soret band with comparable intensities. In **2** and **4**, the effective conjugation can be expected between the porphyrin and the phenylethynyl substituent but the steric interaction causes a significant tilt of the peripheral porphyrin with respect to the phenyl bridge. Thus the placement of the transition dipole moments as shown in Scheme 3B is appropriate for consideration of their absorption spectra. M_y aligned to the long axis of the trimers is larger than M_x and is coupled strongly with m_y and the coupling of M_x and m_z should be much weaker. Consequently, the red-shifted transition would be more intense than blue-shifted transition and is probably covering the small blue-shifted transition. In these cases also, the bandwidth of the Soret bands of the peripheral porphyrins and central diphenylethynyl-substituted porphyrin are spread as a result of the exciton coupling. The observed distinct spectral changes such as red shift and intensification of the Q-bands in **2** and **4** imply the stronger electronic couplings than those in **1** and **3**.

The comparison of the S_1-S_1 energy transfer rate constants among these four trimer systems indicates their strong correlation with the electronic coupling which is determined by connectivity of the central diphenylethynyl-linked porphyrin. As mentioned above, the ground-state absorption in the Q-bands of the central porphyrin showed red shift by the introduction of the peripheral porphyrins in **2** and **4**, while it was scarecely affected in **1** and **3**. These results may be interpreted from the viewpoints of the π-conjugation among trimers which is related to the conformation of the spacers. In **1** and **3**, the 1,4-phenylene

TABLE 2: Summary of Energy Transfer in Benzene

	compound			
	1	**2**	**3**	**4**
τ_2/ps[a]	0.15	0.14	0.07	0.12
k_2[b]	6.1×10^{12} s^{-1}	6.4×10^{12} s^{-1}	7.7×10^{12} s^{-1}	1.7×10^{12} s^{-1}
τ_1/ps[c]	1.6	0.45	4.6	0.48
k_1[d]	6.3×10^{11} s^{-1}	2.2×10^{12} s^{-1}	2.2×10^{11} s^{-1}	2.1×10^{12} s^{-1}
τ_1/ps[e]	1.4−1.6	0.45−0.56	4.5−5.5	0.75−0.80
k_1[f]	$(6.3-6.7) \times 10^{11}$ s^{-1}	$(1.8-2.2) \times 10^{12}$ s^{-1}	$(1.8-2.2) \times 10^{11}$ s^{-1}	1.3×10^{12} s^{-1}

[a] Fluorescence lifetime of donor S_2. [b] S_2-S_2 energy transfer rate (k_2) determined by eq 2 using the values of τ_{0S2}, 1.4 ps for **1** and **2**, and 0.15 ps for **3** and **4**. [c] Fluorescence lifetime of donor S_1. [d] S_1-S_1 energy transfer rate (k_1) determined by eq 1 using the values of τ_{0S1}, 2.1 ns for **1** and **2**, and 1.45 ns for **3** and **4**. [e] Lifetime of donor S_1 measured by transient absorption spectra. [f] S_1-S_1 energy transfer rate (k_1) determined on the basis of the transient absorption spectra.

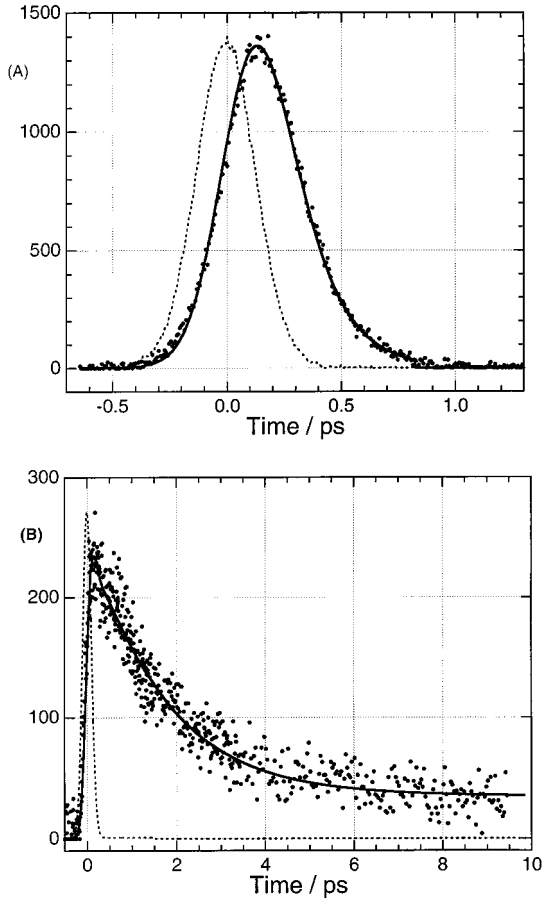

Figure 7. Fluorescence decay profile of **1**; $\lambda_{ex} = 393$ nm, (A) $\lambda_{em} = 460$ nm, (B) $\lambda_{em} = 600$ nm. Dashed line indicates the instrument response.

spacer is prohibited to take planar conformation with respect to the porphyrin plane because of the steric hindrance. The deviation from the planar structure relative to the porphyrins seems to be more pronounced in **3** due to the steric repulsion between the phenylene spacer and the franking peripheral methyl substituents. Thus, the 1,4-phenylene spacer disrupts the effective conjugative interactions between porphyrins. On the other hand, in **2** and **4**, the introduction of the ethynyl group in the bridges may cause less steric hindrance for the phenylene group. Actually, the red-shifted ground-state absorption of the Q-bands of **2** and **4** support the presence of the effective π-conjugation between the central porphyrin and the peripheral moieties through the phenylethynyl spacers. This ground-state absorption spectral changes in **2** and **4** indicate that their S_1-S_1 energy transfer should not be treated in terms of the Förster mechanism alone while the almost unaffected Q-bands in **1** and **3** suggest weaker electronic coupling in their S_1-S_1 energy transfer which may be considered in terms of the Förster mechanism.

Comparison of the models with the same connectivity, **1** vs **3** and **2** vs **4**, is interesting in view of assessment of the molecular orbital effects and thus the relative importance of the through-bond and through-space interactions on the S_1-S_1 energy transfer. The S_1-S_1 energy transfer proceeds with similar rate in **2** and **4** but is faster in **1** than **3**. It is well established that OEP-type Zn(II) porphyrins have a_{1u} HOMO orbital and TPP-type Zn(II) porphyrins have a_{2u} HOMO orbital.[21,40] The a_{2u} orbital has substantial electron density on the *meso*-carbon atoms, where the 1,4-phenylene spacer is appended, while the a_{1u} orbital has negligible electron density at the *meso*-positions. This leads to an expectation for faster energy transfer in TPP-type Zn(II)-porphyrin than OEP-type porphyrin appended to spacer via the *meso*-position, as extensively studied by Lindsey, Holten, and Bocian.[21] Therefore, nearly the same energy transfer rates in **2** and **4** suggest smaller contribution of such molecular orbital effects via through-bond interaction.

On the basis of eqs 3 and 4, we have calculated the Förster energy transfer rate in **1** and **3** as follows; the spectral overlap integrals are estimated from the absorption spectrum of **5** and the fluorescence spectrum of an energy donor porphyrin monomer. In the numerical calculation, we used the values of 0.049 and 0.029 for Φ, and 2.10 and 1.45 ns for τ of **6** and **7**, respectively. The center-to-center distance, R, has been estimated to be 12.5 Å by semiempirical MO calculation.[41] As to the orientation factors (κ^2), we only consider the Q-transition along the diphenylethynyl-substitution direction, since they almost constitute the energy-accepting transition dipole moments.[42] Therefore, the orientation factor is at most 1 for **1** and **3**. The spectral overlap integrals are calculated to be 2.2×10^{-13} cm^6 mmol^{-1} for the both trimers, and the Förster energy transfer rate constants are calculated to be quite similar, 2.3×10^{11} and 2.0×10^{11} s^{-1} for **1** and **3**, respectively. The calculated Förster energy transfer rate is nearly the same as the experimentally observed rate in **3**. This equality may be incidental but it can be said that the electronic interaction must be the minimum in **3** due to its unfavorable connectivity and the OEP-type energy donor that is unfavorable for through-bond electronic interactions. Deviation between the observed and calculated S_1-S_1 energy transfer rate for **1** suggests the substantial contribution of the through-bond electronic interaction.

One of the major findings is the considerably shortened lifetime of the peripheral porphyrin S_2-state, which suggests the occurrence of the S_2-S_2 energy transfer from the peripheral porphyrin to the central diphenylethynyl porphyrin. Normally internal conversions of S_2-states to S_1-states are quite rapid and the energy-transfer reactions from S_2-states are rather difficult to occur due to their extremely short lifetimes. As noted above, however, TPP-type Zn(II) porphyrins have relatively long-lived

TABLE 3: Fluorescence Decay Curve Analyses (Picoseconds)[a]

compound		decay analyses			
1	λ_{ex} (nm)	410		420	
	λ_{em} (nm)	460	500	600	710
		0.050 (−0.90)	0.075 (−0.95)	0.075 (0.51)[b]	0.20 (−0.57)
		0.15 (1.00)	0.15 (1.00)	0.15 (−0.19)[b]	1.5 (−0.12)[b]
				1.7 (0.43)	2000 (1.00)[b]
				2000 (0.07)[b]	
2	λ_{ex} (nm)	393		420	
	λ_{em} (nm)	450	500	600	710
		0.14 (1.00)	0.08 (−0.99)	0.14 (−0.92)	0.13 (−0.27)
			0.10 (1.00)	0.45 (0.72)	0.45 (−0.60)[b]
				2.0 (0.19)	5.8 (0.25)
				2000 (1.00)[b]	2000 (1.00)[b]
3	λ_{ex} (nm)	393		420	
	λ_{em} (nm)	430	470	590	710
		0.07 (1.00)	0.07 (−0.97)	0.10 (−0.61)	0.07 (−0.48)[b]
			0.13 (1.00)	1.2 (0.59)	0.13 (0.01)[b]
				4.6 (0.41)	4.6 (−0.50)[b]
					2000 (0.99)[b]
4	λ_{ex} (nm)	393		420	
	λ_{em} (nm)	450	500	585	710
		0.017 (−1.00)	0.10 (−0.89)	0.10 (0.80)[b]	0.30 (−0.76)
		0.12 (1.00)	0.12 (1.00)[b]	0.12 (−0.64)[b]	0.50 (−0.24)[b]
				0.48 (0.20)	2000 (1.00)[b]
				2000 (0.00)[b]	

[a] Values in parentheses are the relative amplitudes in multiexponential function. [b] Lifetime components were fixed during deconvolution.

S_2-states (2−3 ps), being favorable for S_2-S_2 energy transfer. The S_2-S_2 energy transfer has been also suggested for **3** and **4** on the basis of the shortened lifetime of the peripheral porphyrin S_2-state but is difficult to substantiate due to the intrinsic extremely short S_2-lifetime of the OEP-type energy donor.

Close proximity of the donor and acceptor is prerequisite to the S_2-S_2 energy transfer. Moreover, strongly dipole-allowed transitions to S_2-state (Soret-transition) of both the peripheral porphyrin donors and the central porphyrin acceptor should be responsible for the present energy transfer. The Coulombic interaction (U_{ij}) depends on the magnitude of the transition dipole moments as written by eq 5.

$$U_{ij} = \frac{\mathbf{m}_1 \cdot \mathbf{m}_2 \cdot - 3(\mathbf{m}_1 \cdot \mathbf{e}) \times (\mathbf{m}_2 \cdot \mathbf{e})}{4\pi\epsilon_0 R^3} \qquad (5)$$

In general, Soret bands of porphyrins have large oscillator strength and the mutual Coulombic interactions of these strongly dipole-allowed transitions may lead to large electronic coupling. Simple estimation on the basis of the relative magnitudes of the oscillator strength has provided ca. 9 times large Coulombic interaction for the S_2-S_2 energy transfer versus the S_1-S_1 energy transfer in the model **1**. Obviously, these electronic coupling causes the spectral changes in the Soret bands of both the donor and acceptor in **1**−**4**. Under these conditions, the Soret bands of the donors and acceptors were observed at different wavelength, indicating that the S_2-states are strongly perturbed but retain their identities. The latter feature is crucial for the state-to-state energy transfer and relatively large differences between the S_2-state excitation energy (0.19−0.27 eV, Table 1) are also important for the present S_2-S_2 energy transfer not only for the reaction exothermicity but also for avoidance of the exciton case. Finally, large spectral overlap between the TPP-type Zn(II) porphyrin donor and the diphenylethynyl-linked Zn-(II) porphyrin acceptor is also favorable for the S_2-S_2 energy transfer (Figure 8).

In contrast to the S_1-S_1 energy transfer, the rate constants of the S_2-S_2 energy transfer are similar for **1** and **2**. This implies that the through-space Coulombic interaction is dominant in the

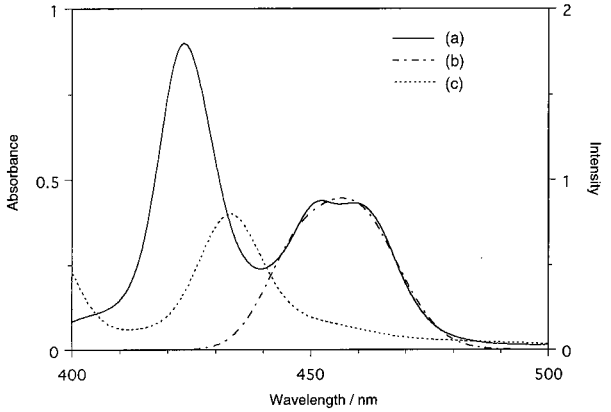

Figure 8. Spectral overlap in S_2-S_2 energy transfer in **1** in benzene. (a) Absorption spectrum of **1**. (b) Calculated Soret band of **1**. (c) Fluorescence spectrum of **6**.

S_2-S_2 energy transfer. In other words, the S_2-S_2 energy transfer in these trimeric porphyrin arrays is mainly facilitated by the extremely large Coulombic interaction provided by the strong Soret absorption bands. Under such conditions the electronic exchange interactions, which are a function of the connectivity and the identity of the donor porphyrin (TPP vs OEP), would play only a minor role.

Other curious findings are the distinct bleachings of the peripheral porphyrin donors in the transient absorption spectra of **3** and **4** at 20 ps delay time (Figures 5C,D). Such indications were also noted for the spectra of **1** and **2** (Figure 5A,B). In line with these results, a long-lived luminescent component from the peripheral porphyrin was commonly detected for **1**−**4** (Figure 7B and Supporting Information).[43]

In conclusion, we demonstrated that the energy-transfer reactions proceed from the peripheral porphyrin to the central diphenylethynyl-substituted porphyrin in both the S_1-state and S_2-state manifolds. Strongly dipole-allowed S_0-S_2-transitions of the porphyrin donors and porphyrin acceptor make a state-to-state S_2-S_2 energy transfer effective enough to compete with the very fast internal conversion to the S_1-state. *meso*-Ethynyl-substituted porphyrin unit is an excellent energy accepting unit

in view of its easy synthetic accessibility and the very efficient energy transfer from TPP- and OEP-type porphyrins both in the S_1- as S_2-states. Incorporation of these functional subunits into more sophisticated supramolecular porphyrin arrays will be an interesting next target that is actively pursued in our laboratories.

Experimental Section

General. Spectra-grade solvents were used for all the spectroscopic measurements. UV−vis absorption spectra were recorded on a Shimadzu UV-2400PC spectrometer. Steady-state fluorescence emission spectra were recorded on a Shimadzu RF-5300PC spectrofluorometer.

Picosecond transient absorption spectra were measured by means of a microcomputer-controlled laser photolysis system with a custom-built repetitive mode-locked Nd^{3+}:YAG laser.[29] The second harmonic of the Nd^{3+}:YAG laser at 532 nm with 15 ps fwhm was used for excitation. For the detection with higher time resolution, dual OPA femtosecond laser system was employed. The output of Ti:Sapphire oscillator (65 fs fwhm, 800 nm, 800mW, 82 MHz) is regeneratively amplified. This amplified pulse (90 fs fwhm, 1W, 1 kHz) is divided into two pulses with the same energy and guided into the OPA systems. By using several nonlinear crystals, the OPA can cover the wavelength region from 300 nm to 3 μm with the output energy of a few to several tens of μJ/pulse. One of the two OPA systems is used for the pump light source and the other for the probe pulse. The output energy of the probe pulse was reduced to $<$1/1000. The pulse duration estimated by the cross-correlation between the pump and probe pulses at the sample position was 160 fs. Sample solutions with $10^{-4}-10^{-5}$ M concentration were used for the transient absorption measurements after nitrogen gas bubbling.

Determination of the energy transfer rates has been done using a femtosecond fluorescence up-conversion method based on a Ti:sapphire laser (Spectra Physics, tsunami, 840 nm, 80 MHz) which was pumped with diode-pumped solid-state laser (Spectra Physics, Millennia X).[32] A second harmonics of a Ti:sapphire laser at 390−420 nm was used for the excitation laser pulse. To avoid polarization effects, the angle between the polarizations of the excitation and probe beams were set to the magic angle by a 1/2λ plate. The instrumental response function had a width of 200 fs (fwhm). Sample solutions were degassed by repeated freeze−pump−thaw cycles just prior the measurements.

The synthetic procedures and physical properties of the new compounds in this paper are given in Supporting Information.

Acknowledgment. This work was supported by Grant-in-Aids for Scientific Research (Grants 11136221 and 11223205) from the Ministry of Education, Science, Sports and Culture of Japan, and by CREST (Core Research for Evolutional Science and Technology) of Japan Science and Technology Corporation (JST).

Supporting Information Available: The synthetic procedures and physical properties of the compounds **1**−**5, 7**−**18**, **21**, and **23**−**25**. This material is available free of charge via the Internet at http://pubs.acs.org.

References and Notes

(1) (a) Wasielewski, M. R. *Chem. Rev.* **1992**, *92*, 435. (b) Wagner, R. W.; Johnson, T. E.; Lindsey, J. S. *J. Am. Chem. Soc.* **1996**, *118*, 11166. (c) Hsiao, J. S.; Krueger, B. P.; Wagner, R. W.; Johnson, T. E.; Delaney, J. K.; Mauzerall, D. C.; Fleming, G. R.; Lindsey, J. S.; Bocian, D. F.; Donohoe, R. J. *J. Am. Chem. Soc.* **1996**, *118*, 11181. (c) Seth, J.; Palaniappan, V.; Wagner, R. W.; Johnson, T. E.; Lindsey, J. S.; Bocian, D. F. *J. Am. Chem. Soc.* **1996**, *118*, 11194. (d) Osuka, A.; Maruyama, K.; Yamazaki, I.; Tamai, N. *Chem. Phys. Lett.* **1990**, *165*, 392. (e) Osuka, A.; Tanabe, T.; Nakajima, S.; Maruyama, K. *J. Chem. Soc., Perkin 2* **1996**, 199.

(2) (a) Gust, D.; Moore, T. A.; Moore, A. L. *Acc. Chem. Res.* **1993**, *26*, 198. (b) Kurreck, H.; Huber, M. *Angew. Chem., Int. Ed. Engl.* **1995**, *34*, 849. (c) Osuka, A.; Mataga, N.; Okada, T. *Pure Appl. Chem.* **1997**, *69*, 797.

(3) (a) Wagner, R. W.; Lindsey, J. S. *J. Am. Chem. Soc.* **1994**, *116*, 9759. (b) Wagner, R. W.; Lindsey, J. S.; Seth, J.; Palaniappan, V.; Bocian, D. F. *J. Am. Chem. Soc.* **1996**, *118*, 3996.

(4) (a) Debreczeny, M. P.; Svec, W. A.; Wasielewski, M. R. *Science* **1996**, *274*, 584. (b) Gosztola, D.; Niemczyk, M. P.; Wasielewski, M. R. *J. Am. Chem. Soc.* **1998**, *120*, 5118.

(5) (a) Osuka, A.; Shimidzu, H. *Angew. Chem., Int. Ed. Engl.* **1997**, *36*, 135. (b) Susumu, K.; Shimidzu, T.; Tanaka, K.; Segawa, H. *Tetrahedron Lett.* **1996**, *37*, 8399. (c) Khoury, R. G.; Jaquinod, L.; Smith, K. M. *Chem. Commun.* **1997**, 1057. (d) Aratani, N.; Osuka, A.; Kim, Y. H.; Jeong, D. H.; Kim, D. *Angew. Chem., Int. Ed.* **2000**, *39*, 1458. (e) Nakano, A.; Yamazaki, T.; Nishimura, Y.; Akimoto, S.; Yamazaki, I.; Osuka, A. *Chem. Eur. J.* **2000**, *6*, 3254.

(6) (a) Martin, R. E.; Diederich, F. *Angew. Chem, Int. Ed.* **1999**, *38*, 1350. (b) Schewab, P. F. H.; Levin, M. D.; Michl, J. *Chem. Rev.* **1999**, *99*, 1863. (c) Vicente, M. G.; Jaquinod, L.; Smith, K. M. *Chem. Commun.* **1999**, 1771. (d) Burrell, A.; Officer, D. L. *Synlett.* **1998**, 1297. (e) Anderson, H. L. *Chem. Commun.* **1999**, 2323. (f) Collman, J. P.; Anson, F. C.; Barnes, C. E.; Bencosme, S. C.; Geier, T.; Evitt, E. R.; Kreh, R. P.; Meier, K.; Pettman, R. B. *J. Am. Chem. Soc.* **1983**, *105*, 2694. (g) Chang, C. K.; Abdalmuhdi, I. *Angew. Chem., Int. Ed. Engl.* **1984**, *23*, 164. (h) Meier, H.; Kobuke, Y.; Kugimiya, S. *J. Chem. Soc., Chem. Commun.* **1989**, 923. (i) Sessler, J. L.; Hugdall, J.; Martin, M. R. *J. Org. Chem.* **1986**, *51*, 2838. (j) Heiler, D.; McLendon, G.; Rogalskyj, P. *J. Am. Chem. Soc.* **1987**, *109*, 604. (k) Osuka, A.; Maruyama, K. *J. Am. Chem. Soc.* **1988**, *110*, 4454. (l) Brun, A. M.; Harriman, A.; Heitz, V.; Savauge, J. P. *J. Am. Chem. Soc.* **1991**, *113*, 8657. (m) Staab, H. A.; Carell, T. *Angew. Chem., Int. Ed. Engl.* **1994**, *33*, 1466. (n) Crossley, M. J.; Burn, P. L. *J. Chem. Soc., Chem. Commun.* **1991**, 1569. (o) Segawa, H.; Kunimoto, K.; Susumu, K.; Taniguchi, M.; Shimidzu, T. *J. Am. Chem. Soc.* **1994**, *116*, 11193. (p) Dubowchik, G. M.; Hamilton, A. D. *J. Chem. Soc., Chem. Commun.* **1987**, 293. (q) Drain, C. M.; Lehn, J.-M. *J. Chem. Soc., Chem. Commun.* **1994**, 2313. (r) Stang, P. J.; Fan, J. Olenyuk, B. *Chem. Commun.* **1997**, 1453. (s) Mongin, O.; Papamicaël, C.; Hoyler, N.; Gossauer, A. *J. Org. Chem.* **1998**, *63*, 5568. (t) Mak, C. C.; Bampos, N.; Sanders, J. K. M. *Angew. Chem., Int. Ed. Engl.* **1998**, *37*, 3020. (u) Sugiura, K.; Tanaka, H.; Matsumoto, T.; Kawai, T.; Sakata, Y. *Chem. Lett.* **1999**, 1193. (v) Higuchi, H.; Shinbo, M.; Usuki, M.; Takeuchi, M.; Hasegawa, Y.; Tani, K.; Ojima, J. *Bull. Chem. Soc. Jpn.* **1999**, *72*, 1887. (x) Kariya, N.; Imamura, T.; Sasaki, Y. *Inorg. Chem.* **1997**, *36*, 833.

(7) (a) Osuka, A.; Tanabe, N.; Kawabata, S.; Yamazaki, I.; Nishimura, T. *J. Org. Chem.* **1995**, *60*, 7177. (b) Osuka, A.; Ikeda, M.; Shiratori, H.; Nishimura, Y.; Yamazaki, I. *J. Chem. Soc., Perkin Trans. 2* **1999**, 1029. (c) Harriman, A.; Ziessel, R. *Chem. Commun.* **1996**, 1707 and references therein. (d) Kilsa, K.; Kajanus, J.; Martensson, J.; Albinsson, B. *J. Phys. Chem. B* **1999**, *103*, 7329.

(8) Hofmann, E.; Wrench, P. M.; Sharples, F. P.; Hiller, R. G.; Welte, W.; Diederichs, K. *Science* **1996**, *272*, 1788.

(9) (a) McDermott, G. M.; Prince, S. M.; Freer, A. A.; Lawless, A. H. H.; Papiz, M. Z.; Cogdell, R. J.; Isaacs, N. W. *Nature* **1995**, *374*, 517. (b) Koepke, J.; Hu, X.; Muenke, C.; Schulten, K.; Michel, H. *Structure* **1996**, *4*, 581. (c) Pullerits, T.; Sundström, V. *Acc. Chem. Res.* **1996**, *29*, 381. (d) Sundström, V.; Pullerits, T.; van Grondelle, R. *J. Phys. Chem. B* **1999**, *103*, 2327. (e) van Oijen, A. M.; Ketelaars, M.; Köhler, J.; Aartsma, T. J.; Schmidt, J. *Science* **1999**, *285*, 400.

(10) van Grondelle, R.; Dekker, J. P.; Gillbro, T.; Sundström, V. *Biochim. Biophys. Acta* **1994**, *1187*, 1.

(11) (a) Gust, D.; Moore, T. A.; Moore, A. L.; Devadoss, C.; Liddel, P. A.; Hermant, R.; Nieman, R. A.; Demanche, L. J.; DeGraziano, J. M.; Gouni, I. *J. Am. Chem. Soc.* **1992**, *114*, 3590. (b) Debreczeny, M. P.; Wasielewski, M. R.; Shinoda, S.; Osuka, A. *J. Am. Chem. Soc.* **1997**, *119*, 6407. (c) Krueger, B. P.; Scholes, G. D.; Jimenez, R.; Fleming, G. R. *J. Phys. Chem. B* **1998**, *102*, 2284.

(12) (a) Kobayashi, H.; Kaizu, Y. In *Porphyrins*: *Excited States and Dynamics*; Gouterman, M., Rentzepis, P., Straub, K., Eds.; American Chemical Society Symposium Series 321; American Chemical Society: Washington, DC, 1986; p 105. (b) Chosrowjan, H.; Taniguchi, S.; Okada, T.; Takagi, S.; Arai, T.; Tokumaru, K. *Chem. Phys. Lett.* **1995**, *242*, 644.

(13) (a) Guzadyan, G. G.; Tran-Thi, T.-H.; Gustavsson, T. *J. Chem. Phys.* **1998**, *108*, 385. (b) LeGourriérec, D.; Andersson, M.; Davidsson, J.; Mukhtar, E.; Sun, L.; Hammarström, L. *J. Phys. Chem. A* **1999**, *103*, 557. (c) Andersson, M.; Davidsson, J.; Hammarström, Korppi-Tommola, J.; Peltola, T. *J. Phys. Chem. B* **1999**, *103*, 3258. (d) Akimoto, S.; Yamazaki, T.; Yamazaki, I.; Osuka, A. *Chem. Phys. Lett.* **1999**, *309*, 177. (e) Cho, H.

S.; Song, N. W.; Kim, Y. H.; Jeoung, S. C.; Hahn, S. J.; Kim, D.; Kim, S. K.; Yoshida, N.; Osuka, A. *J. Phys. Chem. B* **2000**, *104*, 3284.

(14) Harriman, A.; Hissler, M.; Trompette, O.; Ziessel, R. *J. Am. Chem. Soc.* **1999**, *121*, 2516.

(15) (a) Lin, V. S.-Y.; DiMagno, S. G.; Therien, M. J. *Science* **1994**, *264*, 1105. (b) Lin, V. S.-Y.; Therien, M. J. *Chem. Eur. J.* **1995**, *1*, 645. (c) Kumble, R.; Palese, S.; Lin, V. S.-Y.; Therien, M. J.; Hochstrasser, R. M. *J. Am. Chem. Soc*. **1998**, *120*, 11489. (d) LeCours, S. M.; DiMagno, S. G.; Therien, M. J. *J. Am. Chem. Soc.* **1996**, *118*, 11854. (e) Karki, L.; Vance, F. W.; Hupp, J. T.; LeCours, S. M.; Therien, M. J. *J. Am. Chem. Soc.* **1998**, *120*, 2606. (f) LeCours, S. M.; Guan, H.-W.; DiMagno, S. G.; Wang, C. H.; Therien, M. J. *J. Am. Chem. Soc.* **1996**, *118*, 1497. (g) LeCours, S. M.; Philips, C. M.; de Paula, J. C.; Therien, M. J. *J. Am. Chem. Soc.* **1997**, *119*, 12578.

(16) (a) Arnold, D. P.; Johnson, A. W.; Mahendran, M. *J. Chem. Soc., Perkin 1* **1978**, 366. (b) Arnold, D. P.; Nitschinsk, L. J. *Tetrahedron* **1992**, *48*, 8781.

(17) (a) Milgrom, L. R.; Yahioglu, G. *Tetrahedron Lett.* **1995**, *36*, 9061. (b) Milgrom, L. R.; Yahioglu, G. *Tetrahedron Lett.* **1996**, *37*, 4069. (c) Milgrom, L. R.; Rees, R.; Yahioglu, G. *Tetrahedron Lett.* **1997**, *38*, 4905.

(18) (a) Anderson, H. L. *Inorg. Chem.* **1994**, *33*, 972. (b) Taylor, P. L.; Wylie, A. P.; Huuskonen, J.; Anderson, H. L. *Angew. Chem., Int. Ed. Engl.* **1998**, *37*, 986. (c) Taylor, P. N.; Huuskonen, J.; Rumbles, G.; Aplin, R. T.; Williams, E.; Anderson, H. L. *Chem. Commun*. **1998**, 909. (d) Wilson, G. S.; Anderson, H. L. *Chem. Commun*. **1999**, 1539.

(19) (a) Yeoung, M.; Ng, A. C. H.; Drew, M. G. B.; Vorpagel, E.; Breitung, E. M.; MaMahon, R. J.; Ng, D. K. P. *J. Org. Chem.* **1998**, *63*, 7143. (b) Schultz, D. A.; Lee, H.; Gwaltney, K. P. *J. Org. Chem.* **1998**, *63*, 7584. (c) König, B.; Zieg, H. *Synthesis* **1998**, 171. (d) Chen, C.-T.; Yeh, H.-C.; Zhang, X.; Yu, J. *Org. Lett.* **1999**, *1*, 1767. (d) Higuchi, H.; Ishikawa, T.; Miyabayashi, K.; Miyake, M.; Yamamoto, K. *Tetrahedron Lett.* **1999**, *40*, 9091. (e) Odobel, F.; Suzenet, F.; Blart, E.; Quintard, J.-P. *Org. Lett.* **2000**, *2*, 131.

(20) Nakano, A.; Shimidzu, H.; Osuka, A. *Tetrahedron Lett.* **1998**, *39*, 9489.

(21) (a) Strachan, J. P.; Gentermann, S.; Seth, J.; Kalsbeck, W. A.; Lindsey, J. S.: Holten, D.; Bocian, D. F. *J. Am. Chem. Soc.* **1997**, *119*, 11191. (b) Strachan, J. P.; Gentermann, S.; Seth, J.; Kalsbeck, W. A.; Lindsey, J. S.; Holten, D.; Bocain, D. F. *Inorg. Chem.* **1998**, *37*, 1191. (c) Yang, S. I.; Lammi, R. K.; Seth, J.; Riggs, J. A.; Arai, T.; Kim, D.; Bocain, D. F.; Holten, D.; Lindsey, J. S. *J. Phys. Chem. B* **1998**, *102*, 9426. (d) Hascoat, P.; Yang, S. I.; Lammi, R. K.; Alley, J.; Bocian, D. F.; Lindsey, J. S.; Holten, D. *Inorg. Chem.* **1999**, *38*, 4849. (e) Yang, S. I.; Seth, J.; Balasubramanian, T.; Kim, D.; Lindsey, J. S.; Holten, D.; Bocian, D. F. *J. Am. Chem. Soc*. **1999**, *121*, 4008.

(22) Tabushi, I.; Kugimiya, S.; Kinnaird, M. G.; Sasaki, T. *J. Am. Chem. Soc.* **1985**, *107*, 4192.

(23) Lindsey, J. S.; Schreiman, I. C.; Hsu, H. C.; Kearney, P. C.; Marguerettaz, A. M. *J. Org. Chem*. **1987**, *52*, 827.

(24) DiMagno, S. G.; Lin, S.-Y.; Therien, M. J. *J. Org. Chem.* **1993**, *58*, 5983.

(25) (a) Wang, Q. M.; Bruce, D. W. *Synlett.* **1995**, 1267. (b) Littler, B. J.; Miller, M. A.; Hung, C.-H.; Wagner, R. W.; O′Shea, D. F.; Boyle, P. D.; Lindsey, J. S. *J. Org. Chem.* **1999**, *64*, 1391.

(26) Takahashi, S.; Kuroyama, Y.; Sonogashira, K.; Hagihara, N. *Synthesis* **1980**, 627.

(27) The analogous coupling reactions with 5, 15-dibromo porphyrin gave lower yields of **2** and **4** (ca. 20−25%) along with more amounts of **23** and **25** (50−60%).

(28) Seybold, P. G.; Gouterman, M. *J. Mol. Spectrosc.* **1969**, *31*, 1.

(29) Miyasaka, H.; Moriyama, T.; Itaya, A. *J. Phys. Chem.* **1996**, *100*, 12609.

(30) Rodriguez, J.; Kirmaier, C.; Holten, D. *J. Am. Chem. Soc.* **1989**, *111*, 6500.

(31) Osuka, A.; Nakajima, S.; Maruyama, K.; Mataga, N.; Asahi, T.; Yamazaki, I.; Nishimura, Y.; Ohno, T.; Nozaki, K. *J. Am. Chem. Soc.* **1993**, *115*, 4577.

(32) (a) Akimoto, S.; Takaichi, S.; Ogata, T.; Nishimura, Y.; Yamazaki, I.; Mimuro, M. *Chem. Phys. Lett.* **1996**, *260*, 147. (b) Akimoto, S.; Yamazaki, I.; Takaichi, S.; Mimuro, M. *Chem. Phys. Lett.* **1999**, *313*, 63.

(33) Since the excitation wavelength corresponds to the high energy edge of the Soret band, inclusion of a rise component with a shorter time constant was reported to lead to better fitting analysis (ref 13a).

(34) It is possible to analyze the fluorescence decay data on the basis of the Scheme 4. Rigorously, we might consider other processes including vibrational relaxation and solvent dynamics in these fast time region but such processes are not explicitly included in Scheme 4. The rate equations can be expressed in the following forms: $d[D(S_2)]/dt = -\lambda_1[D(S_2)]$, $\lambda_1 = k_{D2f} + k_2 + k_{D2}$ (6); $d[A(S_2)]/dt = k_2[D(S_2)] - \lambda_2[A(S_2)]$, $\lambda_2 = 2k_{21} + k_{A2f} + k_{A2}$ (7); $d[D(S_1)]/dt = k_{D2}[D(S_2)] + k_{21}[A(S_2)] - \lambda_3[A(S_1)]$, $\lambda_3 = k_{D1f} + k_{D1} + k_1$ (8); and $d[A(S_1)]/dt = k_{A2}[A(S_2)] + k_1[D(S_1)] - \lambda_4[A(S_1)]$, $\lambda_4 = k_{A1f} + k_{A1}$ (9) where $[D(S_2)]$, $[D(S_1)]$, $[A(S_2)]$, and $[A(S_1)]$ are the concentrations of the donor and acceptor molecules in the S_2- and S_1-state, respectively, and k's are the rate constants indicted in Scheme 4. The general solutions of the differential eqs 6−9 can be obtained as follows: $[D(S_2)] = a_1e^{-\lambda_1 t}$ (10), $[A(S_2)] = b_1e^{-\lambda_1 t} + b_2e^{-\lambda_2 t}$ (11), $[D(S_1)] = c_1e^{-\lambda_1 t} + c_2e^{-\lambda_2 t} + c_3e^{-\lambda_3 t}$ (12), and $[A(S_1)] = d_1e^{-\lambda_1 t} + d_2e^{-\lambda_2 t} + d_3e^{-\lambda_3 t} + d_4e^{-\lambda_4 t}$ (13). Assuming that the fluorescence at 450−460, 500, 600, and 710 nm are mainly coming from the S_2- and S_1-states of the donor and acceptor, respectively, we have calculated the rate constants, k_1, k_2, and k_{21} 6.3×10^{11} and 2.2×10^{12} s^{-1}, 6.1×10^{12} and 6.6×10^{12} s^{-1}, 5.6×10^{12} and 5.5×10^{12} s^{-1}, for **1** and **2** by substituting the fluorescence lifetimes into eqs 10−13. Successful analysis of this treatment is also consistent with the occurrence of the S_2-S_2 energy transfer.

(35) (a) Kasha, M. *Radiat. Res.* **1963**, *20*, 55. (b) Kasha, M.; Rawls, H. R.; El-Bayoumi, M. A. *Pure Appl. Chem.* **1965**, *11*, 371.

(36) Förster, T. *Discuss. Faraday Soc.* **1959**, *27*, 7.

(37) (a) Kakitani, T.; Kimura, A.; Sumi, H. *J. Phys. Chem. B* **1999**, *103*, 3720. (b) Kimura, A.; Kakitani, T.; Yamato, T. *J. Phys. Chem. B* **2000**. In press.

(38) Dexter, D. L. *J. Chem. Phys.* **1953**, *21*, 836.

(39) (a) Lin, S. H.; Xiao, W. Z.; Dietz, W. *Phys. Rev. E* **1993**, *47*, 47. (b) Newton, M. *Chem. Rev.* **1991**, *91*, 767. (c) Scholes, G. D.; Ghiggino, K. P.; Oliver, A. M.; Paddon-Row, M. N. *J. Phys. Chem.* **1993**, *97*, 11871. (d) Jordan, K. D.; Paddon-Row, M. N. *Chem. Rev.* **1992**, *92*, 395. (e) Clayton, A. H. A.; Scholes, G. D.; Ghiggino, K. P.; Paddon-Row, M. N. *J. Phys. Chem.* **1996**, *100*, 10912 and references therein.

(40) (a) Gouterman, M. *J. Mol. Spectrosc.* **1961**, *6*, 138. (b) Longuest-Higgins, H. C.; Rector, C. W.; Platt, J. R. *J. Chem. Phys.* **1950**, *18*, 1174. (c) Fajer, J.; Davis, M. S. In *The Porphyrins*; Dolphin, D., Ed.; Academic Press: New York, 1979; Vol. 4, Chap 4. (d) Barzilay, C. M.; Sibilia, S. A.; Spiro, T. G.; Gross, Z. *Chem. Eur. J.* **1995**, *1*, 222.

(41) The calculation was performed by MOPAC 97 (AM1) on Chem3D Pro (Version 5.0, Cambridge Soft Co.).

(42) For **5**, Therien et al. have calculated the oscillator strength of Q_x-transition ca. 9 times larger than that of Q_y-transition.

(43) Although we do not have clear explanation for these observations at the present stage, these facts may indicate that the S_1-S_1 energy transfer is accompanied by some photochemical event such as an approach to an equilibrium between the S_1-states of the donor and acceptor, as suggested by one of the referees, or formation of delocalized excited state over the donor and acceptor porphyrins.